ISSN 2616-5775 Vol. 8, Issue 5: 55-63, DOI: 10.25236/AJCIS.2025.080506

Application of Extreme Learning Machine for Land Use Identification

Yuan Zhang[1,*], Xinghong He[1], Xiyan Yang[2]

[1]*College of Hydraulic and Architectural Engineering, Tarim University, Alar City, China*
[2]*College of Information Engineering, Tarim University, Alar City, China*
**Corresponding author*

Abstract: *With the rapid evolution of global land use patterns, accurate and efficient land use identification technologies are crucial for resource management and ecological protection. This study focuses on the application of the Extreme Learning Machine (ELM) in land use identification and systematically conducts a sensitivity analysis of Landsat bands. By constructing an ELM classification model, we quantify the contribution of each band and band combination to the recognition accuracy of different land use types. The results indicate that the ELM model exhibits excellent performance in land use identification, achieving an overall identification accuracy of 80.9% when the number of hidden neurons is set to 90. The sensitivity analysis reveals that bands B3, B4, and B7 demonstrate significant advantages in desert identification, consistently maintaining an accuracy of 100%. Bands B5 and B7 achieve an accuracy of 99% in water identification, while identifying construction land presents the main challenge, with an average accuracy of only 54.7%. The further introduction of vegetation indices (e.g., EVI, NDVI) and band combination analysis shows that EVI enhances the recognition accuracy of forest land by 29.3%, and NDWI improves the recognition accuracy of construction by 10%. This verifies the important value of band sensitivity analysis in optimizing feature selection.This study confirms that band sensitivity analysis based on ELM can effectively reveal the intrinsic correlations between spectral data and land use types, providing a scientific basis for constructing high-precision and robust land use identification models, which is significant for advancing the application of remote sensing technology in land resource monitoring and management.*

Keywords: *Extreme Learning Machine; Land Use; Band Sensitivity Analysis*

1. Introduction

Scene classification of remote sensing images is crucial for various fields, including land management, urban planning, environmental exploration and monitoring, and natural disaster detection[1-2]. Over the past few decades, researchers have conducted extensive experiments in scene classification for satellite and aerial photographs, leading to the development of numerous taxonomies[3]. However, most classical methods rely on artificial or shallow learning algorithms, which extract low- to mid-level semantic features with limited descriptive capability. This limitation hinders further improvements in classification accuracy. Machine learning (ML) has become instrumental in addressing challenging problems in forecasting, classification, and clustering. However, conventional machine learning algorithms typically assume that the underlying distributions of training and testing samples are the same. Unfortunately, this assumption is frequently violated in practice, causing conventional ML algorithms to fall short of their intended purpose [4]. The extreme learning machine (ELM), introduced by Huang et al., is a relatively new algorithm that has been applied to various relational problems due to its simple structure, rapid learning capabilities, and superior generalization performance[5].

Currently, numerous domestic and international scholars have applied Extreme Learning Machines (ELM) to the classification of remote sensing images, achieving commendable results. However, most studies focus on high-resolution images[6-7]. The challenge lies in the fact that many high-resolution remote sensing images lack long-term sequences and are difficult to obtain, resulting in a scarcity of research on the classification of medium and low-resolution remote sensing images using ELM. To address this gap, we propose a novel automatic recognition system for remote sensing images based on Landsat imagery with a resolution of 30m×30m. By investigating the sensitivity of ELM to the bands of Landsat TM remote sensing images and understanding the interaction and disturbance mechanisms

ISSN 2616-5775 Vol. 8, Issue 5: 55-63, DOI: 10.25236/AJCIS.2025.080506

inherent to the ELM model, this study aims to provide a theoretical foundation for the recognition and classification of remote sensing images utilizing ELM. Additionally, we evaluate the effects of various band indices, including DVI, RVI, NDVI, NDWI, and EVI, on the accuracy of predicting forest land, grassland,farmland, construction land, water, and desert areas.

2. Materials and Methods

2.1 Data processing

The artificial feature sample data consists of 200 samples, collected from the Aksu region. Given that neural network models require a substantial number of samples for effective training, an additional 2200 sample points were interpreted from Google Earth images with a resolution of 0.9 meters during the same period. The coordinate information and feature types of these points were recorded, and they will be utilized alongside the artificial feature sample data for training the neural network. The feature types include forest land, grassland,farmland, water, construction land, and desert, as illustrated in Fig. 1. The Landsat 1-7 TM remote sensing image data were sourced from the Landsat series available on the Geospatial Data Cloud, with a resolution of 30 meters (strip numbers 144/145/146/147, line numbers 31/32). The Landsat remote sensing images from the same period underwent geometric correction, atmospheric correction, geometric calibration, radiometric calibration, and image mosaic stitching and cropping. Ultimately, band values and indices for 2400 sample pixels were extracted, including EVI, DVI, RVI, NDVI, and NDWI.

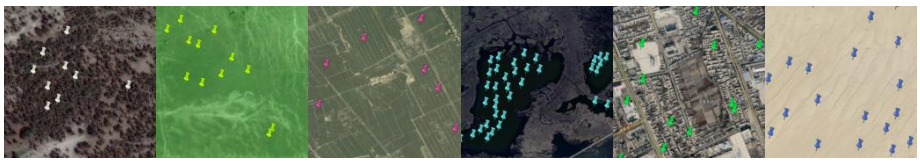

Figure 1 Remote Sensing Interpretation Samples

(Note: from left to right are forest , grassland, farmland, water, construction and desert)

2.2 Extreme learning machine(ELM)

Extreme Learning Machine (ELM) is characterized as a single-hidden layer feedforward network (SLFN). Unlike traditional neural networks, ELM operates in a single step rather than through iterative processes. Consequently, the learning speed of ELM is significantly faster than that of conventional neural networks. In ELM, the parameters, including input weights and hidden biases, are fixed after being randomly generated, allowing the output layer weights to be computed using the least squares solution[8].The basic principle of the extreme learning machine is shown in Figure 2.

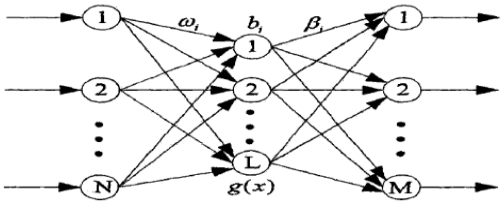

Figure 2 Basic schematic diagram of the extreme learning machine

The mathematical modeling of ELM-based classifier is presented in the following formula in detail. Firstly, we assume the training data specimens $H(Y_n, T_n)$ utilized for designing the ELM classifier then activation function $g(x) = 1/1+e^{-\lambda x}$ will be utilized and is represented as

$$f_i(x_{proc}) = \sum_{i=1}^{h} \beta_i g(\omega_i \cdot x_{proc} + b_i) \tag{1}$$

Where

$$g(\omega_i \cdot x_{proc} + b_i) = \frac{1}{1+e^{-(\omega_i \cdot x_{proc} + b_i)}} \tag{2}$$

ISSN 2616-5775 Vol. 8, Issue 5: 55-63, DOI: 10.25236/AJCIS.2025.080506

For h hidden nodes with G training data specimens and error = zero, then relation of β_i; ω_i and b_i:

$$f_i(x_n) = \sum_{i=1}^{h} \beta_i g(\omega_i \cdot x_n + b_i) = H\beta \tag{3}$$

$$H = \begin{bmatrix} h(x_1) \\ \vdots \\ h(x_G) \end{bmatrix} = \begin{bmatrix} g(\omega_1 \cdot x_1 + b_1) & \cdots & g(\omega_h \cdot x_1 + b_h) \\ \vdots & \ddots & \vdots \\ g(\omega_1 \cdot x_G + b_1) & \cdots & g(\omega_h \cdot x_G + b_h) \end{bmatrix} \tag{4}$$

And β is given by

$$\beta = \begin{bmatrix} \beta_{1,1} & \cdots & \beta_{1,m} \\ \vdots & \ddots & \vdots \\ \beta_{h,1} & \cdots & \beta_{h,m} \end{bmatrix} \tag{5}$$

The output weight vector β can be calculated by

$$\beta = H^{\psi} \cdot T \tag{6}$$

Where H^{ψ} = the Moore–Penrose pseudo-inverse of the hidden layer output matrix H

T = the output matrix is given as follows:

$$T = \begin{bmatrix} t_{1,1} & \cdots & t_{1,m} \\ \vdots & \ddots & \vdots \\ t_{h,1} & \cdots & t_{h,m} \end{bmatrix} \tag{7}$$

Based on this learning algorithm, ELM training was quickly completed.

3. Results and discussions

3.1 ELM-based band sensitivity analysis

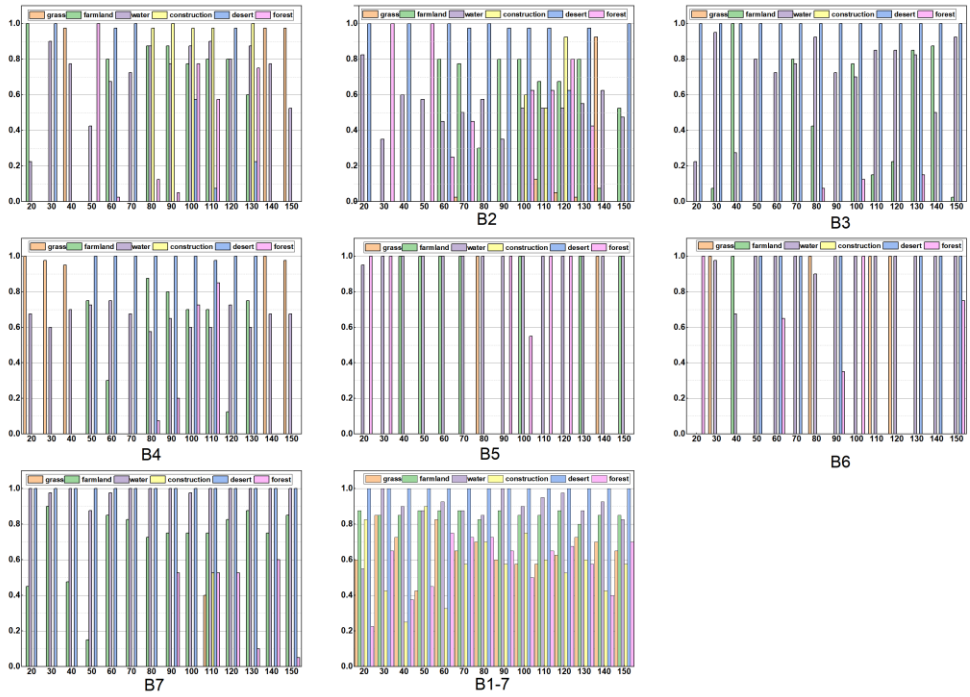

Figure 3 ELM-based band sensitivity analysis

(Note: horizontal coordinate is the number of hidden neurons, vertical coordinate is the inversion accuracy of neural network)

ISSN 2616-5775 Vol. 8, Issue 5: 55-63, DOI: 10.25236/AJCIS.2025.080506

Since the launch of the first satellite in 1972, the Landsat series has accumulated decades of Earth observation data, providing crucial support for global land monitoring. The bands are as follows: Band 1 is the blue light band (0.45-0.52 μm); Band 2 is the green light band (0.52-0.60 μm); Band 3 is the red light band (0.63-0.69 μm); Band 4 is the near-infrared band (0.77-0.90 μm); Band 5 is the short-wave infrared 1 band (1.55-1.75 μm); Band 6 is the thermal infrared band (10.4-12.5 μm); and Band 7 is the short-wave infrared 2 band (2.09-2.35 μm). These seven bands span a broad spectral range from visible to thermal infrared, complementing each other to provide multi-dimensional spectral information for remote sensing applications, such as land use classification, vegetation dynamics monitoring, and the inversion of surface physical parameters. They play a pivotal role in the comprehensive analysis of complex surface environments. To investigate the perturbation mechanism of ELM land use type classification, this paper employs the ELM model to analyze Landsat remote sensing images across these bands, with the results illustrated in Figure 3.

The results indicate that for the ELM model, the optimal number of hidden neurons ranges from 70 to 120. In terms of single-band sensitivity analysis, the B1 band exhibits the highest sensitivity to water, achieving a maximum recognition accuracy of 90%, which enables effective differentiation between water and soil. The B2 band demonstrates greater sensitivity to deserts and farmland; specifically, with 100 hidden neurons, the recognition accuracy for farmland is 80%, while for deserts, it is 98%. This band can be utilized to assess vegetation presence and health. The B3 band is notably sensitive to both deserts and water, consistently identifying deserts with an accuracy of 100%, regardless of the number of hidden neurons, while achieving 80% accuracy for water bodies. Thus, the ELM can distinguish between deserts and non-deserts using the B3 band as a key feature, which is crucial for differentiating between vegetated and non-vegetated areas. The B5 band also shows high sensitivity to water bodies, maintaining a 100% recognition accuracy irrespective of the number of hidden neurons, allowing for a complete distinction between water bodies and non-water bodies based solely on the B5 band. Similarly, the B6 band is highly sensitive to water bodies, achieving a recognition accuracy of 99%. The B7 band is sensitive to deserts, water bodies, andfarmland, with recognition accuracies of 100% for deserts, 99% for water bodies, and 71% for farmland, making it the band that best reflects feature information among the B1 to B7 bands.

Overall, bands B3, B4, and B7 demonstrate a remarkable capability to identify deserts without the limitations typically associated with neurons, achieving a recognition accuracy approaching 100%. This makes deserts the least ambiguous category among the features analyzed. Bands B5 and B7 also exhibit high efficacy in recognizing water bodies, with individual recognition accuracy nearing 100%. However, the overall recognition accuracy for water bodies declines to 88.9% when integrating bands. In contrast, the individual bands are less effective in classifying and recognizing grassland, forest, and construction areas. Nevertheless, following band integration, the recognition accuracy improves to 65.9%for grassland and 57.5% for forest and construction, likely attributable to the development of multidimensional spectral features and the complementary nature of these features. Bands B1, B2, B4, and B7 can be utilized for identifying arable land, although they are prone to confusion with other land feature classes.

3.2 Sensitivity analysis of vegetation index based on ELM

Vegetation indices reflect the differences in vegetation reflectance between the visible and near-infrared bands, as well as the soil background. Various vegetation indices can effectively quantify the physiological state and cover information of vegetation under specific conditions, providing an intuitive and differentiated basis for land remote sensing monitoring. This study investigates the significance of several common band indices in the inversion of feature identification using the ELM model and explores the potential application value of vegetation indices by integrating machine learning with spectral features. The vegetation indices, including RVI (Ratio Vegetation Index), NDVI (Normalized Vegetation Index), DVI (Difference Vegetation Index), and EVI (Enhanced Vegetation Index), are widely utilized for monitoring vegetation cover, biomass, and growth. Additionally, NDWI (Normalized Difference Water Index) is selected as the water index for identifying water and land boundaries and monitoring the water environment.The calculation formulas and functions of each index are shown in Table 1.

ISSN 2616-5775 Vol. 8, Issue 5: 55-63, DOI: 10.25236/AJCIS.2025.080506

Table 1 Common Band Indices

Index	Formula	Function
RVI(Ratio Vegetation Index)	RVI=NIR/R	The RVI is much higher than 1 for green and healthy vegetation cover areas and about 1 for unvegetated ground, which is suitable for monitoring vegetation growth in areas with high vegetation cover[9].
NDVI(Normalized Vegetation Index)	NDVI=(NIR-R)/(NIR+R)	Usually used to detect the growth status of vegetation; the range of values is from - 1 to 1. When NDVI<0, it means that the ground cover is cloud, water, snow, etc.; when NDVI=0, the ground cover is rock or bare soil, etc.; when NDVI>0, it means that the ground surface is covered with vegetation, and it increases with the increase of the degree of cover[10].
DVI(Difference Vegetation Index)	DVI=NIR-R	It is used for monitoring vegetation ecosystems and is suitable for detecting vegetation in the early to middle stages of vegetation development, or in low to medium cover[11].
EVI(Enhanced Vegetation Index)	$EVI=2.5\times\frac{\rho_{NIR}-\rho_{RED}}{\rho_{NIR}+6\rho_{RED}-7.5\rho_{BLUE}+1}$	Typically used for monitoring in heavily vegetated areas, the vegetation signal is enhanced by the inclusion of a blue band to correct for the effects of soil background and aerosol scattering; EVI values range from - 1 to 1, with a range of 0.2 - 0.8 for green vegetated areas[12].
NDWI(Normalized Difference Water Index)	NDWI=(Green-NIR)/ (Green+ NIR)	Often used to extract water body information from images, suitable for the extraction and monitoring of large water bodies in the natural environment[13].

In this study, a total of 2,400 sample points were extracted, organized, and grouped, with 80% allocated for training and the remaining 20% designated for prediction. The subsequent figure illustrates the impact of incorporating various band indices—DVI, RVI, NDVI, NDWI, and EVI—on the accuracy of predicting forest land, grassland, farmland, construction land, water bodies, and desert areas, under different configurations of hidden neurons. It is noted that both excessively high and low numbers of hidden neurons can adversely affect the accuracy of feature type discrimination. Therefore, this paper selects a range of hidden neurons from 70 to 120 and investigates the influence of band indices on feature classification and recognition, utilizing a constrained learning machine model.

As illustrated in Fig. 4, the model achieves the highest overall recognition performance when the number of hidden neurons is set to 90, resulting in a recognition accuracy of 80.9%. The Extreme Learning Machine demonstrates exceptional recognition accuracy for desert areas, attaining 100% accuracy in desert recognition regardless of variations in the number of hidden neurons or the inclusion of the band index. Conversely, the recognition accuracy for construction land is comparatively lower, with an average recognition accuracy of 54.7%. Data analysis indicates a decreasing trend in recognition accuracy for construction land following the addition of the band index, with a slight improvement observed only upon incorporating the DVI and NDWI indices. Notably, when the number of hidden neurons is set to 120, the combination of B1-7 and NDWI yields the highest recognition accuracy for construction land, reaching 97.5%. The recognition accuracy of the Extreme Learning Machine for water bodies is 91.1%, and the B1-7+ALL combination enhances this accuracy. The average recognition accuracy for grassland using the Extreme Learning Machine is 70.6%. The B1-7+EVI combination improves grassland recognition accuracy by an average of 9.1%, while the B1-7+ALL combination enhances it by an average of 11.2%. For farmland, the average recognition accuracy of the Extreme Learning Machine is notably better, averaging 85.7%. The sensitivity to band indices is minimal, showing no significant fluctuations in recognition accuracy whether or not the band indices are included. The average recognition accuracy for forest land is 72.2%, with a higher sensitivity to the EVI and ALL band indices. The combination of B1-7 and EVI improves accuracy by 29.3%, while the B1-7 and ALL combination enhances accuracy by 23.6% compared to B1-7.

ISSN 2616-5775 Vol. 8, Issue 5: 55-63, DOI: 10.25236/AJCIS.2025.080506

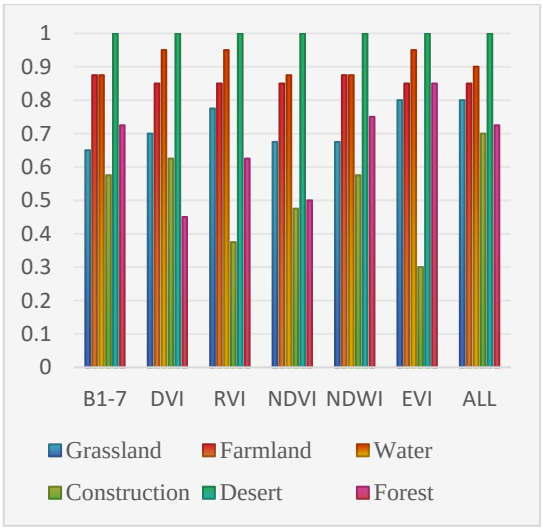

(a)Hidden neurons = 70

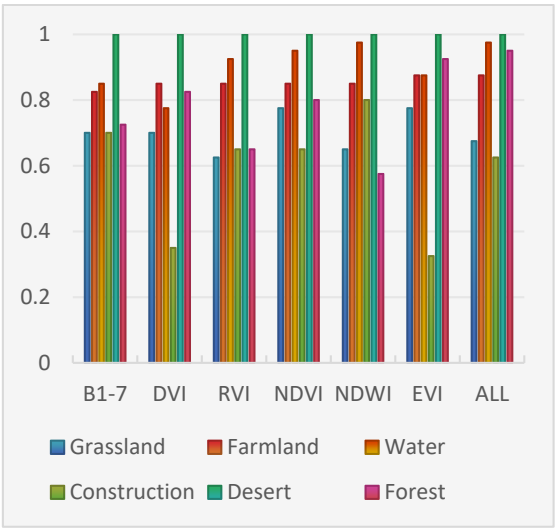

(b)Hidden neurons = 80

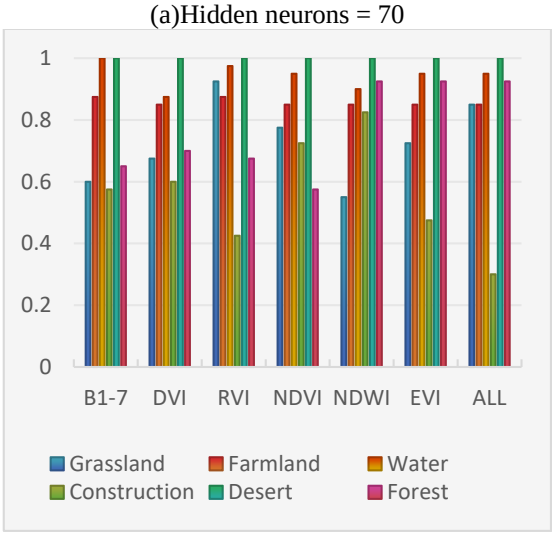

(c)Hidden neurons = 90

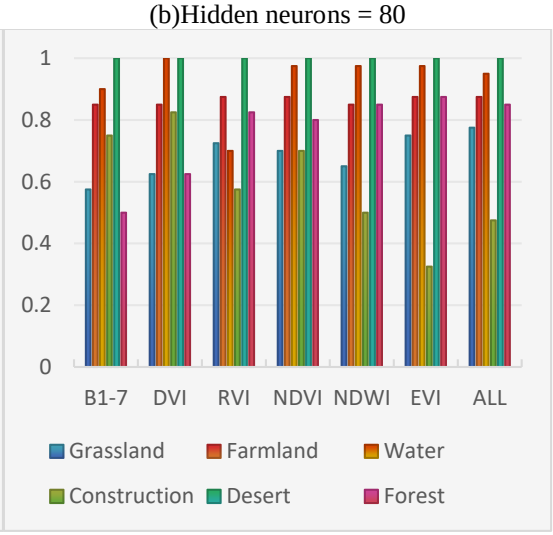

(d)Hidden neurons = 100

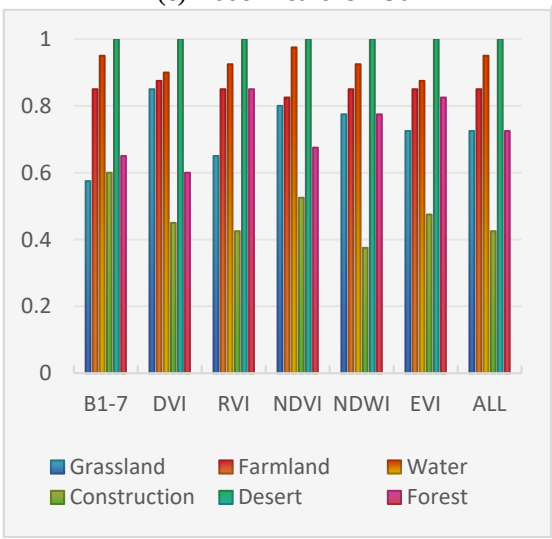

(c)Hidden neurons = 110

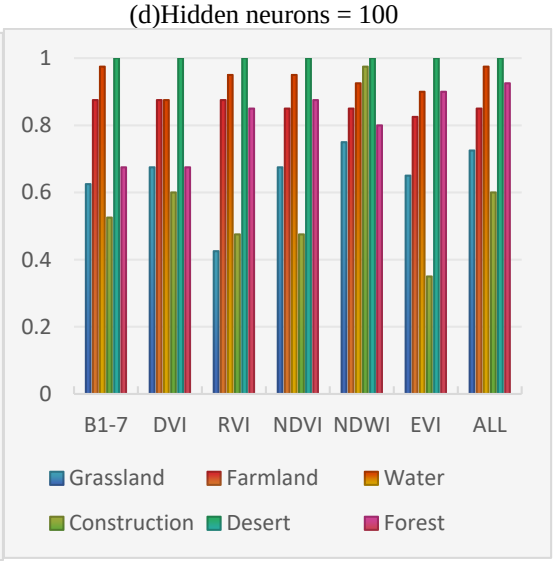

(d)Hidden neurons = 120

Figure 4 Effect of different band indices on feature types under different hidden neuron numbers

ISSN 2616-5775 Vol. 8, Issue 5: 55-63, DOI: 10.25236/AJCIS.2025.080506

Table 2 Classification of the ground objects by the neural network model

	Grassland	Farmland	Water	Construction	Desert	Forest
B1-7	0.659	0.855	0.888	0.575	1.000	0.575
B1-7+DVI	0.668	0.854	0.896	0.611	1.000	0.664
B1-7+RVI	0.689	0.864	0.875	0.500	1.000	0.696
B1-7+NDVI	0.732	0.854	0.936	0.589	1.000	0.707
B1-7+NDWI	0.671	0.850	0.921	0.675	1.000	0.732
B1-7+EVI	0.750	0.861	0.925	0.361	1.000	0.868
ALL	0.771	0.861	0.939	0.518	1.000	0.811

To investigate the sensitivity of the extreme learning machine (ELM) to each band index, the overall recognition accuracy for each hidden neuron was averaged. The results, presented in Table 2, indicate that the overall recognition accuracy for B1-7 is 75.9%, demonstrating greater sensitivity to deserts, water bodies, and farmland, while showing insensitivity to forested land and construction land, which had a recognition accuracy of only 57.5%. After adding the DVI (Difference Vegetation Index), the recognition accuracy of each feature type was improved, and the overall recognition accuracy of B1-7+DVI was 78.2%, of which the most significant improvement in recognition accuracy was for forest land, with the accuracy improved by 8.9%. When the RVI (Ratio Vegetation Index) was added, the overall recognition accuracy for B1-7+RVI reached 77.1%. The RVI specifically improved the recognition accuracy of vegetation types such as grassland, farmland, and forest, with forest land accuracy increasing by 12.1%. However, it had no effect on construction land and water bodies, even reducing their recognition accuracy. The NDVI (Normalized Difference Vegetation Index) significantly improved recognition accuracy for both grassland and forest land, with grassland accuracy increasing by 7.3% and forest accuracy by 13.2%. The overall recognition accuracy for B1-7+NDVI was 80.3%. The NDWI (Normalized Difference Water Index) also greatly enhanced recognition for construction and forest, improving building accuracy by 10% and forest land accuracy by 15.7%, contributing to an overall accuracy increase of 4.97%. The EVI (Enhanced Vegetation Index) significantly boosted accuracy for grassland and forest, with grassland recognition improving by 9.1% and forest by 29.3%.

Overall, the combination of the 7-band values with various band indices resulted in a recognition accuracy that was 5.8% higher than that of the single 7-band, with specific improvements of 11.2% for grassland, 0.6% for farmland, 5.1% for water bodies, and 23.6% for forest land. The highest classification accuracy and optimal results were achieved by utilizing the B1-7 band values alongside all band indices as training objects for the extreme learning machine, leading to an overall accuracy improvement of 5.8%.

3.3 ELM-based land use remote sensing inversion

Extreme Learning Machine (ELM) is particularly well-suited for processing large-scale and high-resolution remote sensing data due to its randomly generated hidden layer parameters, which eliminate the need for iterative optimization. Based on the sensitivity analysis results of ELM concerning Landsat band indices and vegetation indices, this paper utilizes Landsat bands B1, B2, B3, B4, B5, B6, B7, as well as RVI, NDVI, DVI, EVI, and NDWI as the training object limits for the learning machine. The number of hidden neurons is set to 90 for classifying land use in the Alar reclamation area, resulting in an overall model recognition accuracy of 80.9%. The results are illustrated in Figure 5.

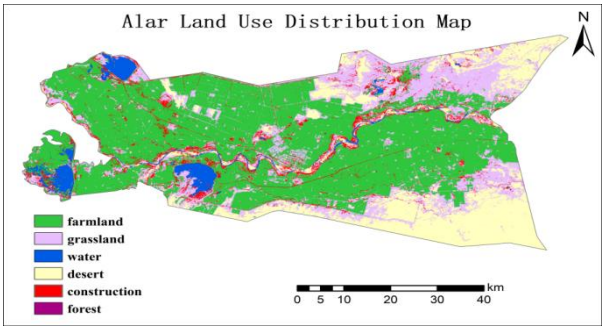

Figure 5 Land use distribution map of Aral

ISSN 2616-5775 Vol. 8, Issue 5: 55-63, DOI: 10.25236/AJCIS.2025.080506

4. Conclusion and discussion

In this paper, we utilize the ELM model to conduct band sensitivity analysis on Landsat remote sensing images, systematically revealing the performance of ELM model parameters and multispectral bands in feature recognition. This study finds that when the number of hidden neurons in the ELM model is within the range of 70 to 120, the overall performance of the model is more stable. Specifically, when the number of hidden neurons is set to 90, the overall recognition accuracy reaches 80.9%, indicating optimal performance and providing a stable algorithmic foundation for subsequent waveband sensitivity analysis.

In terms of single-band sensitivity, each band shows distinctive feature recognition specificity. The results show that Band 1, Band 5, Band 6, and Band 7 have high accuracy in recognizing water bodies even when analyzed individually. These bands can be utilized for monitoring water-related data, such as soil moisture, soil water content, agricultural irrigation management, and drought monitoring. Future research can explore the feasibility of new algorithms and develop new band indices for monitoring subtle plant moisture and crop moisture. Band 3, Band 4, and Band 7 are capable of distinguishing between desert and non-desert areas with a single band, thereby serving as core bands for differentiating vegetation from non-vegetation. Additionally, we can explore new band indices through the combination of these bands to monitor vegetation health, changes in chlorophyll content, and vegetation coverage. The band 2 is particularly sensitive to desert and farmland, making it suitable for monitoring crop growth and providing a foundation for smart agriculture and irrigation practices.

The band indices of RVI, NDVI, DVI, EVI, and NDWI are not significant for the identification of farmland, grassland, desert, and construction land; however, the accuracy of forest land identification has improved, with EVI showing the most significant enhancement, increasing accuracy by 29.3%. This improvement may be attributed to the higher vegetation cover in forested areas, where EVI performs exceptionally well. Furthermore, the fusion of multi-band information provides richer spectral features, aiding in the differentiation of forest from other land cover types. This capability also allows for better capture of details regarding forest vegetation, such as tree species and growth stages, thus offering more multi-dimensional information for forest identification and improving accuracy. Although NDVI, EVI, and NDWI positively influence the recognition accuracy of water bodies, the inclusion of vegetation indices and other bands can reduce the recognition accuracy of water bodies compared to the use of single bands B5 and B7. This reduction may stem from the fact that B5 and B7 belong to the short-wave infrared (SWIR) bands, where water bodies exhibit strong absorption properties and their reflectance approaches zero. In contrast, the reflectance of most non-water features (e.g., vegetation, soil, and construction) is significantly higher in SWIR bands. The underlying reasons for this pronounced spectral difference, which enables the identification of water bodies using a simple reflectance threshold, warrant further investigation.

Acknowledgements

Tarim University Master's Talent Project: Research on Remote Sensing Monitoring and Yield Estimation Model of Cotton in the Alar Irrigation Area Based on Artificial Intelligence (TDZKSS202153).

References

[1] Sekrecka A ,Karwowska K .Classical vs. Machine Learning-Based Inpainting for Enhanced Classification of Remote Sensing Image[J].Remote Sensing,2025,17(7):1305-1305.
[2] Diab M ,Kolokoussis P ,Brovelli A M .Optimizing zero-shot text-based segmentation of remote sensing imagery using SAM and Grounding DINO[J]. Artificial Intelligence in Geosciences, 2025, 6(1):100105-100105.
[3] G. Cheng, P. Zhou, J. Han, et al., Auto-encoder-based shared mid-level visual dictionary learning for scene classification using very high resolution remote sensing images, IET Comput. Vis. 9 (5) (2015) 639–647.
[4] He M , Zhang J ,He Y , et al. Annotated Dataset for Training Cloud Segmentation Neural Networks Using High-Resolution Satellite Remote Sensing Imagery[J].Remote Sensing,2024,16(19):3682-3682. .
[5] G.B. Huang, Q.Y. Zhu, C.K. Siew, Extreme learning machine: theory and applications, Neurocomputing 70 (1-3) (2006) 489–501.
[6] Han M ,Liu B . Ensemble of extreme learning machine for remote sensing image classification [J].

ISSN 2616-5775 Vol. 8, Issue 5: 55-63, DOI: 10.25236/AJCIS.2025.080506

Neurocomputing, 2015, 149 65-70.
[7] Li Q, Peng Q, Chen J, et al. Improving Image Classification Accuracy with ELM and CSIFT[J]. Computing in Science & Engineering, 2018.
[8] G.B. Huang , An insight into extreme learning machines: Random neurons, random features and kernels, Cognit Comput 6 (3) (2014) 376–390 .
[9] Arai K ,Nakaoka Y ,Okumura H .Method for Landslide Area Detection with RVI Data Which Indicates Base Soil Areas Changed from Vegetated Areas[J].Remote Sensing,2025,17(4):628-628.
[10] Meng Z ,Lu Y ,Wang H .Correlation change analysis and NDVI prediction in the Yellow River Basin of China using complex networks and GRNN-PSRLSTM.[J].Environmental monitoring and assessment, 2024, 196(11) :1092.
[11] Wei H Z ,Chen L H ,Zha N F .The Modification of Difference Vegetation Index (DVI) in middle and late growing period of winter wheat and its application in soil moisture inversion[J].E3S Web of Conferences, 2019,13101098.
[12] Huiliang W ,Linpo H ,Jun Y , et al.Effects of Effective Precipitation and Accumulated Temperature on the Terrestrial EVI (Enhanced Vegetation Index) in the Yellow River Basin, China[J]. Atmosphere, 2022,13(10):1555-1555.
[13] Castro D L A ,Duarte L M ,Ewbank H , et al.Use of synthetic aperture radar data for the determination of normalized difference vegetation index and normalized difference water index[J]. Journal of Applied Remote Sensing,2024,18(1):014516-014516.